ANNALS OF GEOPHYSICS, VOL. 52, N. 3/4, June/August 2009

Utilization of antenna arrays in HF systems

Salil D. Gunashekar ([1]), **E. Michael Warrington** ([1]), **Hal J. Strangeways** ([2]), **Yvon Erhel** ([3]), **Sana Salous** ([4]), **Stuart M. Feeney** ([4]), **Nasir M. Abbasi** ([1]), **Louis Bertel** ([5]), **Dominique Lemur** ([5]), **François Marie** ([5]) **and Martial Oger** ([5])

([1]) *Department of Engineering, University of Leicester, UK*
([2]) *School of Electronic and Electrical Engineering, University of Leeds, UK*
([3]) *Centre de Recherches des Ecoles de Saint-Cyr Coetquidan, Guer, France*
([4]) *School of Engineering, Durham University, UK*
([5]) *IETR, Université de Rennes 1, France*

Abstract
Different applications of radio systems are based on the implementation of antenna arrays. Classically, radio direction finding operates with a multi channel receiving system connected to an array of receiving antennas. More recently, MIMO architectures have been proposed to increase the capacity of radio links by the use of antenna arrays at both the transmitter and receiver.
The first part of this paper describes some novel experimental work carried out to examine the feasibility of applying MIMO techniques for communications within the HF radio band. A detailed correlation analysis of a variety of different antenna array configurations is presented. The second section of the paper also deals with HF MIMO communications, focusing on the problem from a modelling point of view. The third part presents a sensitivity analysis of different antenna array structures for HF direction finding applications. The results demonstrate that when modelling errors, heterogeneous antenna arrays are more robust in comparison to homogeneous structures.

Key words *Ionospheric channel – MIMO architecture – array processing – HF channel characterization – superresolution direction finding*

1. Experimental investigations into the feasibility of MIMO techniques within the HF band

1.1. *Introduction*

A multiple input multiple output (MIMO) system utilises antenna arrays at the transmitter as well as receiver ends of a communications link. A rich fading or scattering environment is required for the successful implementation of MIMO, which, in effect, facilitates the creation of multiple paths for the parallel transmission of data. The use of multiple transmitter and multiple receiver antennas in such an environment enables a substantial increase in data rates to be achieved within the same frequency band. For MIMO to be successful however, it is essential that there is sufficient de-correlation between the signals received at each of the antenna elements of the receiver array from each of the elements of the transmitter array.

Signals received over HF (3-30 MHz) propagation paths through the ionosphere are prone to extensive fading as a consequence of multipath and multimode propagation. As such, it would seem that the use of HF signals in a mul-

Mailing address: Prof. E. Michael Warrington, Department of Engineering, University of Leicester, Leicester LE1 7RH, United Kingdom: e-mail: emwarrington@mac.com; emw@leicester.ac.uk

ti-element transmitter-receiver system would be an ideal candidate for the implementation of MIMO techniques. So far, however, apart from the research outlined in Brine *et al.* (2006) and Strangeways (2006a), very little experimental or modelling research has been conducted in this area. Sections 1.2 to 1.4 describe some of the novel experimental work that has been carried out in order to investigate the feasibility of applying MIMO techniques within the HF band.

1.2. *Experimental arrangement and measurements*

In order to carry out HF-MIMO measurements, a purpose-built multi-channel transmitter system and multi-channel receiver system was implemented. The transmitter site was located in Durham, UK, while two receiver sites were utilised in the different campaigns. One receiver site was located in Bruntingthorpe (Leicester), UK (giving a range of approximately 255 km), while the other receiver site was located in Monterfil (Rennes), France (giving a range of approximately 750 km). At present, the system has the capability of transmitting on up to four antennas and receiving on up to eight antennas.

In order to investigate the effects of antenna heterogeneity at the transmitter, a variety of antennas were used in the campaigns (*e.g.* vertical, loop, dipole and crossed-wire antennas). At the receiver, a number of different antenna configurations were employed to demonstrate some of the requirements for the implementation of an effective HF-MIMO system. For example, as reported in Gunashekar *et al*. (2008) and Warrington *et al*. (2008), at times the two orthogonal arms of a spaced *L*-shaped antenna array of vertical monopoles exhibit significantly different levels of de-correlation (as a function of antenna spacing). Furthermore, it has also been confirmed that at HF wavelengths, the use of homogeneous spaced arrays may require significant spacing to achieve acceptable levels of de-correlation (Gunashekar *et al*., 2008 and Warrington *et al*., 2008). In this paper, the results from preliminary investigations that were carried out in order to examine the use of spaced as well as co-located heterogeneous antenna arrays have been presented. The latter would enable the compact implementation of HF-MIMO systems by achieving the necessary de-correlation at a single location.

For the various transmit antennas, slightly different CW frequencies (offset by 10-20 Hz) were used. During testing, it was verified that the different frequencies exhibited correlated fading when transmitted simultaneously on a single antenna. This result confirmed that, when used on separate transmit antennas, the differences in frequencies would not contribute to any kind of de-correlation during the MIMO campaigns.

Over the last several months, a number of experimental campaigns were performed over the Durham-Bruntingthorpe and Durham-Monterfil paths. The following sub-sections provide selected examples of cases in which different MIMO configurations were employed.

1.3. *Spaced, heterogeneous antenna arrays: 4x8 MIMO link between Durham and Monterfil (3 July 2008)*

A 4x8 MIMO configuration was utilised in a series of measurements conducted on 3 July 2008. The transmit array in Durham consisted of the following antennas: TX-1 (5.795010 MHz): N-S arm of an inverted 'V' crossed-wire antenna array (*i.e.* pointing in the general direction of Monterfil), TX-2 (5.795020 MHz): E-W arm of an inverted 'V' crossed-wire antenna array, TX-3 (5.795030 MHz): a loop antenna and TX-4 (5.795040 MHz): a vertical antenna. The receiver configuration in Monterfil comprised of an eight channel heterogeneous circular array of radius 25.0 m. As illustrated in fig. 1, the eight channels were connected to octagonal loop antennas that were arranged so that successive loops were oriented perpendicular to each other.

The amplitude pattern across the eight receiving channels for CW signals received from Durham for a period of approximately one minute (at 10:20 UT on 3 July 2008) depicted deep fading for all four transmissions. This was indicative of the presence of multiple propagation modes/paths. When transmission curves were superimposed on the corresponding verti-

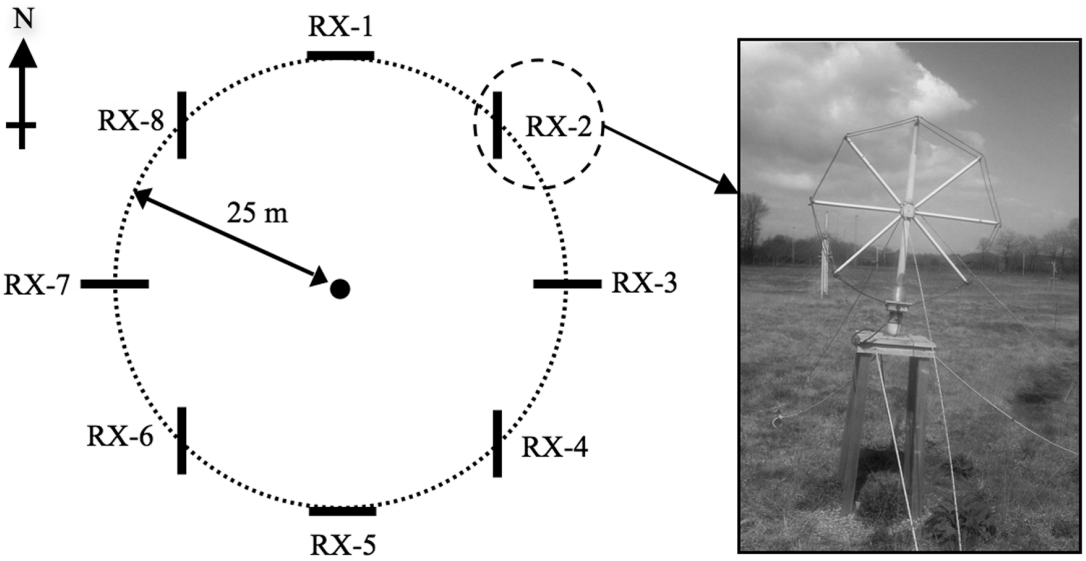

Fig. 1. Heterogeneous circular antenna array (consisting of eight octagonal loop antennas) employed at Monterfil during a 4x8 HF-MIMO campaign on 3 July 2008.

cal ionogram obtained from the Chilton (UK) ionosonde, the presence of multiple propagation modes was confirmed: in addition to the multiple hop *F*2 modes (both ordinary and extraordinary modes), a strong *E*-region was also present.

The magnitudes of the amplitude correlation coefficients between the individual one-minute transmissions at each of the receiving antennas have been listed in table I. The orthogonal nature of the two transmit crossed-wire antennas (TX-1 and TX-2) as well as the antenna diversity present at the transmit end appears to have an implication on the levels of de-correlation achieved at the receiving antennas: approximately 40% and 80% of the values do not exceed 0.7 and 0.9 respectively (according to Loyka (2001), for a 10-element uniform linear array, the MIMO channel capacity does not degrade appreciably until the inter-element correlation coefficient exceeds approximately 0.9).

In addition to the transmissions being reasonably well de-correlated at each of the receiving antennas, the various pairs of receiving antennas were also very well de-correlated for each transmission from Durham. A list of the magnitudes of the amplitude correlation coefficients between the different pairs of receiving antennas of the circular antenna array for TX-1 (N-S inverted 'V' wire antenna; 5.795010 MHz) is presented in table II. A combination of the spatial and heterogeneous nature of the array results in majority of the correlation coefficients lying in the range 0.2-0.8 (and never exceeding approximately 0.85). A similar distribution of correlation coefficients was observed for TX-2, TX-3 and TX-4.

1.4. *Compact, co-located, heterogeneous antenna arrays: 3x5 MIMO link between Durham and Bruntingthorpe (29 July 2008)*

A 3-axis, H-field loop antenna array was designed to investigate the use of co-located heterogeneous antenna arrays at the receiver in Bruntingthorpe. The array consists of three perpendicular active loop antennas mounted on a common mast (height ~3.0 m): two antennas oriented in the N-S and E-W directions and a

Table I. Amplitude correlation coefficients between the various transmissions from Durham at each receiving antenna of the heterogeneous circular antenna array in Monterfil for a period of approximately one minute at 10:20 UT on 3 July 2008 [TX-1: N-S inverted 'V' crossed-wire (5.795010 MHz), TX-2: E-W inverted 'V' crossed-wire (5.795020 MHz), TX-3: loop (5.795030 MHz), TX-4: vertical whip (5.795040 MHz)].

	Magnitude of amplitude correlation coefficients					
	[TX-1, TX-2]	**[TX-1, TX-3]**	**[TX-1, TX-4]**	**[TX-2, TX-3]**	**[TX-2, TX-4]**	**[TX-3, TX-4]**
RX-1	0.61	0.86	0.09	0.84	0.74	0.39
RX-2	0.86	0.95	0.52	0.93	0.74	0.62
RX-3	0.88	0.94	0.46	0.93	0.65	0.58
RX-4	0.94	0.94	0.66	0.94	0.74	0.75
RX-5	0.82	0.90	0.77	0.88	0.82	0.83
RX-6	0.78	0.90	0.53	0.85	0.58	0.53
RX-7	0.85	0.92	0.59	0.88	0.61	0.59
RX-8	0.65	0.84	0.36	0.75	0.46	0.28

Table II. Amplitude correlation coefficients between the various pairs of receiving antennas that constitute the heterogeneous circular antenna array in Monterfil for TX-1 (N-S crossed wire; 5.795010 MHz) for a period of approximately one minute at 10:20 UT on 3 July 2008.

	Magnitude of amplitude correlation coefficients							
	RX-1	**RX-2**	**RX-3**	**RX-4**	**RX-5**	**RX-6**	**RX-7**	**RX-8**
RX-1	-	0.55	0.59	0.37	0.02	0.66	0.49	0.15
RX-2	-	-	0.80	0.02	0.27	0.66	0.70	0.33
RX-3	-	-	-	0.47	0.28	0.81	0.87	0.25
RX-4	-	-	-	-	0.29	0.35	0.36	0.14
RX-5	-	-	-	-	-	0.31	0.35	0.05
RX-6	-	-	-	-	-	-	0.86	0.38
RX-7	-	-	-	-	-	-	-	0.48
RX-8	-	-	-	-	-	-	-	-

horizontal loop antenna. An experimental campaign was conducted on 29 July 2008 that employed the co-located, heterogeneous loop antenna array at the receive end of a 3x5 MIMO link. In addition to this, orthogonally oriented inverted 'V' wire antennas were also employed. Both the inverted 'V' antennas (wire length ~32 m) were supported by the same mast and were crossed at the same point on the mast (approximately 7.6 m above ground level). The N-S arm

of the receive crossed-wire antenna was pointing in the general direction of Durham.

For the transmit array in Durham, three different antennas were utilised: TX-1: N-S arm of an inverted 'V' crossed-wire array (*i.e.* pointing in the direction of Bruntingthorpe), TX-2: E-W arm of an inverted 'V' crossed-wire array and TX-3: a vertical antenna. During the measurement campaign, two sets of transmission frequencies were utilised: 5.255010 MHz (TX-1), 5.255020 MHz (TX-2), 5.255040 MHz (TX-3) (from 11:50 UT to 13:05 UT) and 4.445510 MHz (TX-1), 4.445520 MHz (TX-2), 4.445540 MHz (TX-3) (from 13:15 UT to 14:20 UT).

For each pair of orthogonal active loop antennas, the occurrence frequencies of correlation coefficients that fall within specified bins are presented in fig. 2. The top frame contains the histograms corresponding to the 5.2550 MHz transmissions (54 one-minute data files) while the lower frame corresponds to the 4.4455 MHz transmissions (50 one- minute data files). Particularly for the orthogonal pairs involving the N-S oriented active loop, sufficiently low values of correlation coefficient are observed. Majority of correlation coefficients lie within the range 0.3-0.8 though lower values are also observed for a number of cases. Furthermore, more de-correlation is observed at 5.2550 MHz than at 4.4455 MHz - it is likely that the reduction in wavelength and the prevailing modal structure of the ionosphere are both contributing to this.

Finally, the occurrence frequency histograms of the correlation coefficients between the N-S and E-W receive crossed-wires are depicted in fig. 3 (left frame: 5.2550 MHz; right frame: 4.4455 MHz). For all three transmissions at 5.2550 MHz, the orthogonally-oriented inverted 'V' wire antennas result in adequately low levels of de-correlation (the majority of the correlation coefficients fall within the range 0.4-0.8).

2. Theoretical determination of antenna correlation distances and capacities for HF MIMO links

MIMO systems employ both transmitting and receiving arrays and space-time coding methods in order to achieve significantly greater channel capacities. Since the data rate possible for digital HF systems is generally comparatively low, it would be very useful if the capacity improvements inherent in MIMO techniques could be exploited at HF. In order to assess this possibility and in order to gain some insight into the optimum design of HF MIMO systems, the characteristics of the digital HF channel have been explored in relation to this utilization. To accomplish this a wideband HF simulator, based on a physical model and including time-varying electron density irregularities has been employed and used to assess correlation of the received multi-component signal at spaced antennas for different multipath scenarios and ionosphere parameters (Strangeways, 2005). The optimum parameters and scenarios for employment of HF MIMO systems can then be assessed and capacities and optimum array configurations determined (Strangeways, 2006a,b,c). It needs to be considered that, whereas for the cellular radio case at UHF, the multipath at the receiver can arrive over a wide range of azimuth up to 360 degrees with a small range of elevation, the situation at HF is quite different with all signals arriving from essentially the same azimuth unless refraction occurs from large scale irregularities such as TIDs, gradients in the mid-latitude or high latitude troughs or reflection occurs from patches in the auroral/polar region. However, for the HF case, since paths can result from ionospheric reflection from different layers (*e.g.* E, F) or multi-hops, the range of elevation can be much larger. The effect of time-varying ionospheric irregularities will also result in refracted/diffracted paths which will also decrease the correlation at spaced antennas and also lead to reduced channel stationarity. It also needs to be taken into account that the time scale of the different mechanisms producing multipath at HF vary. Whereas motion of small scale irregularities produce fade periods less than 1s, fading due to interference between reflections from different layers or a different number of hops have longer timescales (up to about 10s).

The correlation distance for spaced antennas, as used in these systems, has been determined using the Leeds-St.Petersburg HF simulator. In this simulator, the channel simulation

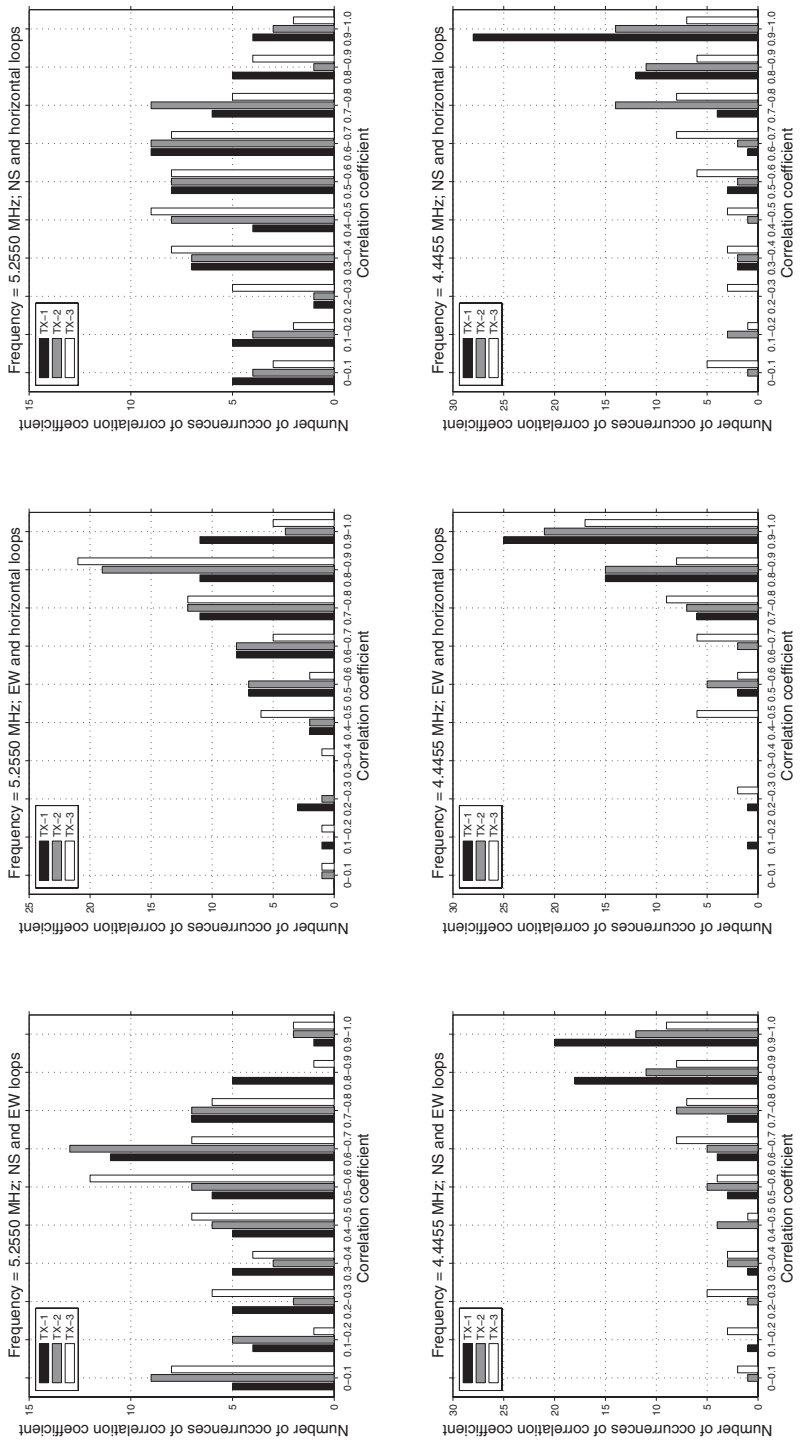

Fig. 2. Correlation coefficient occurrence frequency histograms for each pair of co-located, orthogonal, active loop antennas for each of the transmitting antennas: 3 X 5 MIMO campaign between Durham and Bruntingthorpe on 29 July 2008 [Top frame: 5.2550 MHz transmissions (54 one-minute data files); Lower frame: 4.4455 MHz transmissions (50-one minute data files); TX-1: N-S crossed-wire (5.255010 MHz/4.445510 MHz); TX-2: E-W crossed-wire (5.255020 MHz/4.445520 MHz); TX-3: vertical antenna (5.255040 MHz/4.445540 MHz)].

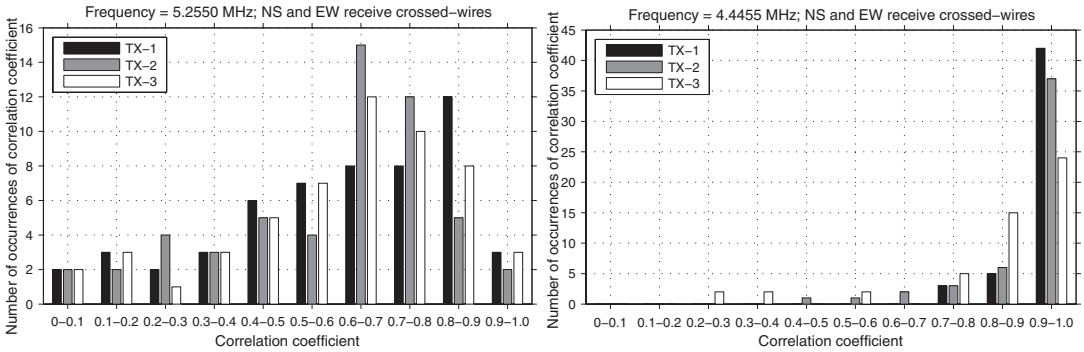

Fig. 3. The occurrence frequency histograms of the correlation coefficients between the N-S and E-W receive crossed wire antennas for each of the transmitting antennas: 3 X 5 MIMO campaign between Durham and Bruntingthorpe on 29 July 2008 [Left frame: 5.2550 MHz transmissions (54 one-minute data files); Right frame: 4.4455 MHz transmissions (50-one minute data files); TX-1: N-S crossed-wire (5.255010 MHz/4.445510 MHz); TX-2: E-W crossed-wire (5.255020 MHz/4.445520 MHz); TX-3: vertical antenna (5.255040 MHz/4.445540 MHz).

for the multipath HF ionospheric sky wave random channel is based on the most general theory of HF wave propagation in the real fluctuating ionosphere (Gherm *et al*., 2005). The complex phase method (or modified Rytov's approximation) is employed. This accounts for the main effects of HF propagation in the disturbed ionosphere: ray bending due to the inhomogeneous background ionosphere and scattering by random ionospheric irregularities including diffraction by localised inhomogeneities. The Earth's magnetic field effect on the irregularity shape is taken into account through the anisotropic spatial spectrum of the ionospheric turbulence. The propagation paths are determined using a Nelder-Mead homing-in algorithm together with a 3D ray-tracing model which takes into account the effect of the geomagnetic field on the refractive index and also permits horizontal gradients of electron density to be included. This enables simulation of the multimoded wideband ionospheric HF channel for both background and stochastic (time-varying irregularities) electron density components for any transmitter and receiver locations and taking into account both magneto-ionic modes for all the ionospherically reflected paths.

The wideband HF simulator can output realisations of the received signal at the receiver in both fast (time-of-flight) and slow time. This can also enable correlation between spaced antennas to be determined assuming frozen-in drift of the irregularities. For antennas spaced in the direction of irregularity velocity drift, for spacings up to a few wavelengths, it was assumed that the spatial variation of the received signal can be modelled in the drift direction using the simulated slow time variation and the known drift velocity. Based on a simple model of scattering from an inhomogeneous and time-varying ionosphere, a spatial correlation function p(d) normalised to unity at d=0 may be derived to show the dependence of CW signals at two antennas spaced by

$$p(d) = e^{\left(-d^2/2\sigma_l^2\right)} \tag{2.1}$$

At a separation d = σ_l the correlation is 0.61 and at d = $\sqrt{2}\sigma_l$, it is 0.37. This latter distance is termed the *diversity separation distance* or *correlation distance* (ITU-R, 1990).

As an example, a North South path from 50° to 62° latitude at 0 ° longitude in the IRI Ionosphere with an East-West drift of the irregularities of 0.5 km/s has been considered. The carrier frequency is 9 MHz and the signal bandwidth is 20 kHz. The standard deviation of the relative

electron density fluctuations, σ_{N2}, is $2x10^{-5}$. The outer scale of the irregularities is 5 km in the transverse direction and 15 km in the geomagnetic field direction. The spectral index is given by p =3.7. The *E* and *F* layer reflected paths exist for both magneto-ionic modes and all 4 paths are included to determine the signal strength at the receiver location (fig. 4). The left frame of fig. 4 shows the received pulse (*E* and *F* modes) in both fast and slow time and the right frame shows how the correlation coefficient falls of with antenna separation for both modes. It is clear that the fall-off is faster for the *F* mode and thus this mode de-correlates over a shorter distance Note that because of the small number of points, the correlation coefficient has been "unbiassed" at each lag by dividing by the number of products taken in determining it, explaining why the maximum for the *E* mode is not at zero lag. The correlation of multipath ionospherically reflected signals is quite complex and will vary during the duration of a dispersed pulse.

The spatial correlation at the receiving antenna array depends strongly on the variance of the electron density irregularities. Each mode (*e.g.* 1*Eo* or 1*Fx*) shows "fading" due to the time-varying irregularities. Paths reflected from the *F* region generally show poorer correlation at spaced antennas than *E* region reflected paths. This is likely to result from the larger absolute changes in electron density in the *F* as opposed to the *E* layer. Although it might be supposed that correlation between spaced receiving antennas would be appreciably decreased by receiving additional modes this is not necessarily the case; *e.g.* lowering the transmission frequency to enable an additional *E* layer reflection may not decrease appreciably the spatial correlation at the receiver as the *E* layer mode added is likely to show better correlation between the spaced antennas than the *F* mode. Moreover decreasing the carrier frequency to enable the E mode will reduce the SNR which will also result in poorer channel capacity for a SIMO/MIMO link. The capacity of HF MIMO links will also vary for different antenna array sizes, geometries, correlations distances and antenna separations. The fig. 5 shows the estimated capacity for a correlation length of 250 m compared to that of 500 m for a 4x4 MIMO system (Strangeways, 2006c). Calculations have also shown that the capacity of an HF MIMO link for uncorrelated received signals is not found to reduce drastically for correlated signals even when the correlation coefficient between adjacent receiving antennas is quite high (by a factor of 0.88 for 0.8 correlation coefficient and 0.80 for 0.9 correlation coefficient for a 2x2 MIMO system).

3. Sensitivity analysis of the heterogeneous array for direction finding applications

3.1. *Introduction*

Direction finding techniques operate with synchronous acquisitions at the output of an array of sensors and the associated covariance matrix is the relevant information for the most popular high resolution algorithms (Capon, Music, Weighted Subspace Fitting). This work investigates the estimation of angular errors resulting from a perturbation on the steering-vector matrix. These uncertainties on the array response are due, for example, to imprecise positions of the sensors or to a default in the calibration of the electronic circuits connected to each of them.

The expressions of the errors (limited to first order terms) are derived for two different structures of array.

The first is the classical homogeneous array set up with identical sensors. The second is the heterogeneous structure (Erhel *et al*., 2004), set up with different sensors, that we proposed for HF applications in order to make the array sensitive to the incoming polarization. Statistics of the angular errors are computed for the two solutions and indicate a greater robustness of the second structure.

3.2. *Expressions for array processing*

3.2.1. Homogeneous (classical) array

A homogeneous array is set up with NC identical sensors associated with a reference

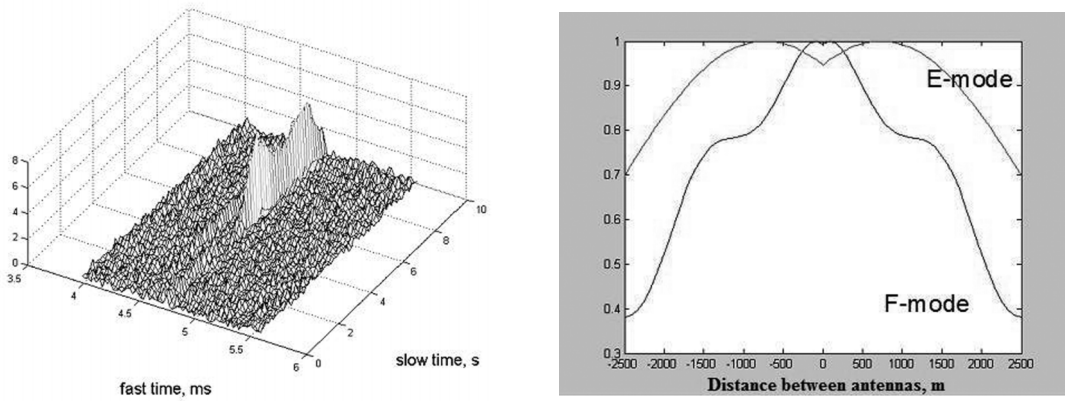

Fig. 4.a,b. Received signal power with added noise for a 9MHz carrier with 20kHz bandwidth and $\sigma_{N2}=2.10^{-5}$ (left frame), and correlation coefficient versus antenna separation for both *E* and *F* modes (right frame).

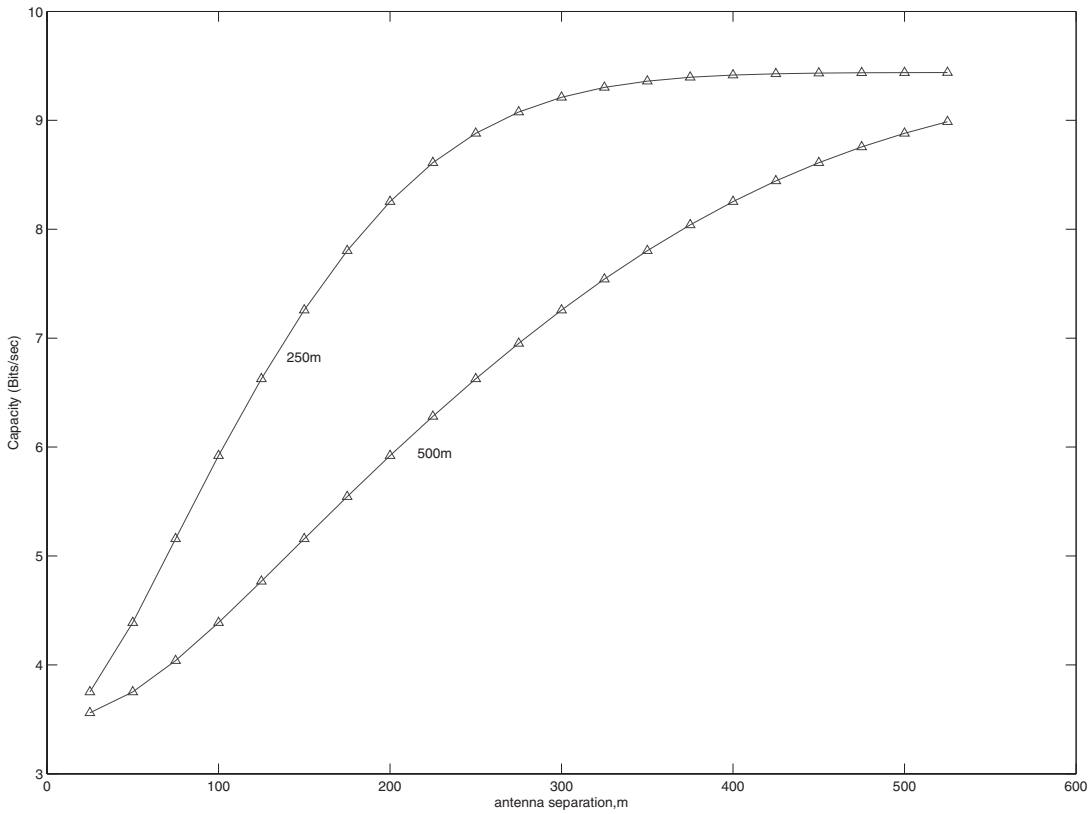

Fig. 5. Capacity achieved for correlation lengths of 250 and 500 m for a 4x4 MIMO system.

point for the geometrical phase. NS waves are assumed to be incident and the corresponding output signals generated on the reference sensor are denoted by $\{s_k(t)\}k=1,..,NS$. Each direction of arrival (DOA) is identified by the angle θ_k (or couple of angles in a 3-D search). For that direction, the geometrical phase between the reference and the n^{th} sensor is denoted by $\varphi_n(\theta_k)$

The output on the n^{th} antenna is expressed as:

$$x_n(t) = \sum_{k=1}^{NS} e^{j\varphi_n(\theta_k)} s_k(t) + n_n(t) \quad (3.1)$$

where the noise components $\{n_n(t)\}$ n=1,...,NC are supposed to be mutually uncorrelated with identical power σ^2 or, equivalently, spatially white.

The NC output signals on the array are collected in the acquisition column vector $\underline{\mathbf{X}}(t)$ as:

$$\underline{\mathbf{X}}(t) = \sum_{k=1}^{NS} \underline{\mathbf{a}}(\theta_k) s_k(t) + \underline{\mathbf{N}}(t) \quad (3.2)$$

where $\underline{\mathbf{a}}(\theta_k)$ is the steering-vector for the D.O.A. θ_k and $\underline{\mathbf{N}}(t)$ is the noise vector.

The components of $\underline{\mathbf{a}}(\theta_k)$ contain the different geometrical phases:

$$\underline{\mathbf{a}}(\theta_k) = \left(e^{j\varphi 1(\theta_k)}, e^{j\varphi 2(\theta_k)}, ..., e^{j\varphi NC(\theta_k)}\right)^T \quad (3.3)$$

Associating the NS steering vectors in the matrix $\mathbf{A}$ provides the classical linear model of acquisitions:

$$\underline{\mathbf{X}}(t) = \mathbf{A}\underline{\mathbf{S}}(t) + \underline{\mathbf{N}}(t) \quad (3.4)$$

where $\underline{\mathbf{S}}(t)$ is the signal vector.

The covariance matrix of the acquisitions, defined as:

$$\mathbf{R_{XX}} = E[\underline{\mathbf{X}}(t).\underline{\mathbf{X}}(t)^H] \quad (3.5)$$

is then expressed as:

$$\mathbf{R_{XX}} = \mathbf{A}\mathbf{R_{ss}}\mathbf{A}^H + s^2\mathbf{Id} \quad (3.6)$$

where $\mathbf{R_{ss}}$ is the covariance of the incident signals:

$$\mathbf{R_{ss}} = E[\underline{\mathbf{S}}(t).\underline{\mathbf{S}}(t)^H] \quad (3.7)$$

3.2.2. Heterogeneous array

A heterogeneous array is made up of sensors which are different from one another. For each of them, the directional gain relatively to the angle θ, called spatial response and denoted by $F_n(\theta)$, n=1,…NC is assumed to be known. Examples of spatial responses for HF antennas with a simple geometry are calculated in (Erhel *et al*., 2004).

The computation refers to a deterministic model of the polarization at the exit point of the ionosphere.

In this context, the linear model for the output signals of the heterogeneous array is expressed as:

$$\underline{\mathbf{X}}_\mathbf{h}(t) = \sum_{k=1}^{NS} \underline{\mathbf{a}}_\mathbf{h}(\theta_k) s_k(t) + \underline{\mathbf{N}}_\mathbf{h}(t) \quad (3.8)$$

The components of the steering-vectors $\underline{\mathbf{a}}_\mathbf{h}(\theta_k)$ combine the spatial responses and the exponentials which represent the phases $\varphi_\mathbf{n}(\theta_\mathbf{k})$ calculated with respect to the array geometry:

$$\underline{\mathbf{a}}_\mathbf{h}(\theta_k) = (F_1(\theta_k)e^{j\varphi 1(\theta_k)}, ..., F_{NC}(\theta_k)e^{j\varphi NC(\theta_k)})^T \quad (3.9)$$

It can be noticed that $\underline{\mathbf{a}}_\mathbf{h}(\theta)$ does not have a constant norm; this remark will be taken into account when applying the MUSIC algorithm on this particular type of array.

Gathering the NS steering-vectors in matrix $\mathbf{A_h}$ gives the linear model for the heterogeneous array:

$$\underline{\mathbf{X}}_\mathbf{h}(t) = \mathbf{A_h}\underline{\mathbf{S}}(t) + \underline{\mathbf{N}}_\mathbf{h}(t) \quad (3.10)$$

and, assuming a spatially white additive noise, the corresponding covariance matrix is

$$\mathbf{R_{xxh}} = \mathbf{A_h}\mathbf{R_{ss}}\mathbf{A_h}^H + \sigma^2\mathbf{Id} \quad (3.11)$$

3.3. *Sensitivity analysis: perturbation method*

Perturbations are assumed to affect the array response: viz random displacements of the sensors or differences in gain and phase for the different acquisition channels connected to the sensors.

However, the assumption of spatially white noise is maintained keeping the noise covariance matrix proportional to the identity matrix.

Consequently, the modified covariance matrix can be written as:

$$\hat{\mathbf{R}}_{\mathbf{xx}} = (\mathbf{A} + \Delta\mathbf{A})\mathbf{R}_{\mathbf{ss}}(\mathbf{A} + \Delta\mathbf{A})^{\mathrm{H}} + \sigma^2\mathbf{Id} \quad (3.12)$$

where $\Delta\mathbf{A}$ is the perturbation of the array matrix due to errors on the manifold.

Several algorithms are based on the eigen decomposition of the covariance matrix $\mathbf{R}_{\mathbf{xx}}$ (Pillai, 1989). The eigen vectors of the noise subspace are the columns of matrix **Vn**. The perturbation of the array manifold induces a variation $\Delta\mathbf{Vn}$ of matrix **Vn**:

$$\hat{\mathbf{V}}_{\mathbf{n}} = \mathbf{V}_{\mathbf{n}} = \mathbf{V}_{\mathbf{n}} + \Delta\mathbf{V}_{\mathbf{n}} \quad (3.13)$$

The noise subspace of the perturbed covariance is characterized by the relation:

$$[(\mathbf{A} + \Delta\mathbf{A})\mathbf{R}_{\mathbf{ss}}(\mathbf{A} + \Delta\mathbf{A})^{\mathrm{H}} + \sigma^2\mathbf{Id}]$$
$$(\mathbf{V}_{\mathbf{n}} + \Delta\mathbf{V}_{\mathbf{n}}) = (\sigma^2\mathbf{Id} + \Delta\Lambda_{\mathbf{n}})(\mathbf{V}_{\mathbf{n}} + \Delta\mathbf{V}_{\mathbf{n}}) \quad (3.14)$$

where $\Delta\Lambda_{\mathbf{n}}$ is the perturbation affecting the diagonal of the noise eigen values.

Developing this expression and assuming that the second order terms can be neglected, we obtain the result (Marcos, 1998):

$$\Delta\mathbf{V}_{\mathbf{n}}^{\mathrm{H}}\mathbf{A} = -\mathbf{V}_{\mathbf{n}}^{\mathrm{H}}\Delta\mathbf{A} \quad (3.15)$$

As a consequence of eq. 3.15, the dependence of the angular error with the perturbation of the array manifold is established in the following section.

The direction finding technique considered as the reference in this work is the MUSIC algorithm (Schmidt, 1986) which estimates the angle of arrival by minimizing relatively to the angular parameter θ the quadratic form:

$$f(\theta) = \underline{\mathbf{a}}^{\mathrm{H}}(\theta)\mathbf{V}_{\mathbf{n}}\,\mathbf{V}_{\mathbf{n}}^{\mathrm{H}}\,\underline{\mathbf{a}}(\theta) \quad (3.16)$$

3.3.1. Homogeneous array

In absence of perturbations, the quadratic form is minimum for the exact angles of arrival:

$$f'(\theta_k) = \frac{df(\theta)}{d\theta}_{\theta=\theta k} = 0 \text{ and } V_n^H\underline{\mathbf{a}}(\theta) = 0 \text{ for } k = 1,.....,NS \quad (3.17)$$

With perturbations, the quadratic form is modified in:

$$\hat{f}(\theta) = \underline{\mathbf{a}}^{\mathrm{H}}(\theta)(\mathbf{V}_{\mathbf{n}} + \Delta\mathbf{V}_{\mathbf{n}})(\mathbf{V}_{\mathbf{n}} + \Delta\mathbf{V}_{\mathbf{n}})^{\mathrm{H}}\underline{\mathbf{a}}(\theta) \quad (3.18)$$

and reaches its minimums for angles equal to:

$$\hat{\theta}_k = \theta_k + \Delta\theta_k \quad (3.19)$$

where $\Delta\theta_{\mathrm{k}}$ is the angular error.

For these values of angle, we can show that:

$$\hat{f}'(\hat{\theta}_k) = 0 = \hat{f}'(\theta_k) + \Delta\theta_k\hat{f}''(\theta_k) + O(\Delta\theta_k^2) \quad (3.20)$$

if the terms of second order are neglected. Besides,

$$\hat{f}'(\theta) = \underline{\mathbf{a}}'^{\mathrm{H}}(\theta)\hat{\mathbf{V}}_{\mathbf{n}}\hat{\mathbf{V}}_{\mathbf{n}}^{\mathrm{H}}\underline{\mathbf{a}}(\theta) + \underline{\mathbf{a}}^{\mathrm{H}}(\theta)\hat{\mathbf{V}}_{\mathbf{n}}\hat{\mathbf{V}}_{\mathbf{n}}^{\mathrm{H}}\underline{\mathbf{a}}'(\theta) \quad (3.21)$$

where $\underline{\mathbf{a}}'(\theta) = \frac{d\underline{\mathbf{a}}(\theta)}{d\theta}$ denotes the derivative of the steering-vector with respect to the angle θ.

The two elements of the sum are conjugated so that:

$$\hat{f}'(\theta) = 2\Re\mathrm{e}\left[\underline{\mathbf{a}}'^{\mathrm{H}}(\theta)\hat{\mathbf{V}}_{\mathbf{n}}\hat{\mathbf{V}}_{\mathbf{n}}^{\mathrm{H}}\underline{\mathbf{a}}(\theta)\right]$$
$$= 2\Re e\left[\underline{\mathbf{a}}'^{\mathrm{H}}(\theta)(\mathbf{V}_{\mathbf{n}} + \Delta\mathbf{V}_{\mathbf{n}})(\mathbf{V}_{\mathbf{n}} + \Delta\mathbf{V}_{\mathbf{n}})^{H}\underline{\mathbf{a}}(\theta)\right] \quad (3.22)$$

This function is calculated for $\theta = \theta_{\mathrm{k}}$ keeping in mind that $\mathbf{V}_{\mathbf{n}}^{\mathrm{H}}\underline{\mathbf{a}}(\theta_{\mathrm{k}}) = 0$ and that the only first order terms in $\Delta\mathbf{V}_{\mathbf{n}}$ are significant.

We get:

$$\hat{f}'(\theta_k) = 2\Re\mathrm{e}\left[\underline{\mathbf{a}}'^{H}(\theta_k)\mathbf{V}_{\mathbf{n}}\mathbf{V}_{\mathbf{n}}^{H}\underline{\mathbf{a}}(\theta_k) + \underline{\mathbf{a}}'^{H}(\theta_k)\mathbf{V}_{\mathbf{n}}\Delta\mathbf{V}_{\mathbf{n}}^{H}\underline{\mathbf{a}}(\theta_k) + \mathbf{a}'^{H}(\theta_k)\Delta\mathbf{V}_{\mathbf{n}}\mathbf{V}_{\mathbf{n}}^{H}\underline{\mathbf{a}}(\theta_k)\right] \quad (3.23)$$

and finally :

$$\hat{f}'(\theta_k) = 2\Re\mathrm{e}\left[\underline{\mathbf{a}}'^{H}(\theta_k)\mathbf{V}_{\mathbf{n}}\Delta\mathbf{V}_{\mathbf{n}}^{H}\underline{\mathbf{a}}(\theta_k)\right] \quad (3.24)$$

The second derivative of the modified quadratic form is expressed as:

$$\hat{f}''(\theta) = \underline{\mathbf{a}}''^{H}(\theta)\hat{\mathbf{V}}_{\mathbf{n}}\hat{\mathbf{V}}_{\mathbf{n}}^{H}\underline{\mathbf{a}}(\theta) + 2\underline{\mathbf{a}}'^{H}(\theta)\hat{\mathbf{V}}_{\mathbf{n}}\hat{\mathbf{V}}_{\mathbf{n}}^{H}\underline{\mathbf{a}}'(\theta) + \underline{\mathbf{a}}^{H}(\theta)\hat{\mathbf{V}}_{\mathbf{n}}\hat{\mathbf{V}}_{\mathbf{n}}^{H}\underline{\mathbf{a}}''(\theta) \quad (3.25)$$

with $\underline{\mathbf{a}}''(\theta) = \dfrac{d^2\underline{\mathbf{a}}(\theta)}{d\theta^2}$ denoting the second derivative of the steering-vector with respect to θ.

Its value, calculated for $\theta = \theta_k$, contains only one zero order term:

$$\hat{f}''(\theta_k) \approx 2\underline{\mathbf{a}}'^H(\theta_k)\mathbf{V_n}\mathbf{V_n}^H\underline{\mathbf{a}}'(\theta_k) \quad (3.26)$$

An approximate expression of the angular error is then:

$$\Delta\theta_k \approx \frac{-\Re e\left[\underline{\mathbf{a}}'^H(\theta_k)\mathbf{V_n}\Delta\mathbf{V_n}^H\underline{\mathbf{a}}(\theta_k)\right]}{\underline{\mathbf{a}}'^H(\theta_k)\mathbf{V_n}\mathbf{V_n}^H\underline{\mathbf{a}}'(\theta_k)} \quad (3.27)$$

and, using the relation showed in eq. 3.15, we finally obtain (Marcos, 1998):

$$\Delta\theta_k \approx \frac{\Re e\left[\underline{\mathbf{a}}'^H(\theta_k)\mathbf{V_n}\mathbf{V_n}^H\Delta\underline{\mathbf{a}}(\theta_k)\right]}{\underline{\mathbf{a}}'^H(\theta_k)\mathbf{V_n}\mathbf{V_n}^H\underline{\mathbf{a}}'(\theta_k)} \quad (3.28)$$

In this relation, the angular error $\Delta\theta_k$ depends on the uncertainty affecting the steering-vector $\underline{\mathbf{a}}(\theta_k)$.

Since the perturbation $\Delta\underline{\mathbf{a}}(\theta_k)$ is a random vector, the angular error is quantified with its statistics. Therefore, we now calculate the mean square error of the angle of arrival.

Denoting $\underline{\mathbf{f_k}} = \mathbf{V_n}^H\underline{\mathbf{a}}'(\theta_k)$, the angular error $\Delta\theta_k$ is written as:

$$\Delta\theta_k = \frac{\underline{\mathbf{f}}_k^H\mathbf{V_n}^H\Delta\underline{\mathbf{a}}(\theta_k) + \Delta\underline{\mathbf{a}}(\theta_k)^H\mathbf{V_n}\underline{\mathbf{f}}_k}{2\underline{\mathbf{f}}_k^H\underline{\mathbf{f}}_k} \quad (3.29)$$

Then, the related mean square error is calculated as:

$$E\left[\Delta\theta_k^2\right] = \frac{\Re e\left\{\underline{\mathbf{f}}_k^H\mathbf{V_n}^H\left(\mathbf{C_{kk}}\mathbf{V_n}\underline{\mathbf{f}}_k + \mathbf{D_{kk}}\mathbf{V_n}^*\underline{\mathbf{f}}_k^*\right)\right\}}{2\underline{\mathbf{f}}_k^H\underline{\mathbf{f}}_k^2} \quad (3.30)$$

where matrices $\mathbf{C_{kk}} = \mathrm{E}\left[\Delta\underline{\mathbf{a}}(\theta_k)\Delta\underline{\mathbf{a}}(\theta_k)^H\right]$ and $\mathbf{D_{kk}} = \mathrm{E}\left[\Delta\underline{\mathbf{a}}(\theta_k)\Delta\underline{\mathbf{a}}(\theta_k)^T\right]$ contain statistics of the perturbation $\Delta\mathbf{a}(\theta_k)$.

3.3.2. Heterogeneous array

In this section, we derive the calculation of the angular error resulting from a perturbed array response $\Delta\mathbf{A_h}$ of a heterogeneous structure.

The modified acquisition covariance matrix is expressed as:

$$\hat{\mathbf{R}}_{\mathbf{xxh}} = (\mathbf{A_h} + \Delta\mathbf{A_h})\mathbf{R_{ss}}(\mathbf{A_h} + \Delta\mathbf{A_h})^H + \sigma^2\mathbf{Id} \quad (3.31)$$

Similarly to relation showed in eq. 3.15, it can be demonstrated that the corresponding perturbation $\Delta\mathbf{V_n}$ of the noise subspace verifies:

$$\Delta\mathbf{V_n}^H\mathbf{A_h} = -\mathbf{V_n}^H\Delta\mathbf{A_h} \quad (3.32)$$

The MUSIC algorithm is based on the orthogonality between the steering-vector of an incident signal and the noise subspace (Schmidt, 1986). As a consequence of implementation operating with an estimation of the covariance matrix, the corresponding vectors are only approximately orthogonal. For this reason, the variable vector to be projected in the noise subspace should have a constant norm for all directions of arrival under test. This condition is obviously fulfilled for the homogeneous array with a norm of $\underline{\mathbf{a}}(\theta)$ being equal to $\sqrt{NC}$ whatever the angle of arrival.

On the contrary, the steering-vector of the heterogeneous array does not have this property as indicated in Section 3.2.2. Therefore, the quadratic form to be minimized in this case is written as (Erhel, 2004):

$$f(\theta) = \underline{\mathbf{b}}_\mathbf{h}^H(\theta)\mathbf{V_n}\mathbf{V_n}^H\underline{\mathbf{b}}_\mathbf{h}(\theta) \quad (3.33)$$

where

$$\underline{\mathbf{b}}_\mathbf{h}(\theta)\underline{\mathbf{a}}_\mathbf{h}(\theta)/\left\|\underline{\mathbf{a}}_\mathbf{h}(\theta)\right\| \quad (3.34)$$

is the normalized steering-vector. Actually, the measure of orthogonality between a variable vector and a given subspace implies that the vector has a constant norm.

The angular error for the heterogeneous array is expressed as an equivalent of relation of eq. 3.27:

$$\Delta\theta_k \cong \frac{-\Re e\left[\underline{\mathbf{b}}_\mathbf{h}'^H(\theta_k)\mathbf{V_n}\Delta\mathbf{V_n}^H\underline{\mathbf{b}}_\mathbf{h}(\theta_k)\right]}{\underline{\mathbf{b}}_\mathbf{h}'^H(\theta_k)\mathbf{V_n}\mathbf{V_n}^H\underline{\mathbf{b}}_\mathbf{h}'(\theta_k)} \quad (3.35)$$

where $\underline{\mathbf{b}}_\mathbf{h}'(\theta) = \dfrac{d\underline{\mathbf{b}}_\mathbf{h}(\theta)}{d\theta}$ is the derivative of the normalized steering-vector relatively to the angle of arrival.

To take benefit of relation of the eq. 3.32, we express that:

$$\Delta \mathbf{V}_n^H \underline{\mathbf{b}}_h(\theta_k) = \Delta \mathbf{V}_n^H \frac{\underline{\mathbf{a}}_h(\theta_k)}{\left\| \underline{\mathbf{a}}_h(\theta_k) \right\|} = -\mathbf{V}_n^H \frac{\Delta \underline{\mathbf{a}}_h(\theta_k)}{\left\| \underline{\mathbf{a}}_h(\theta_k) \right\|} \quad (3.36)$$

to finally obtain the expression of the angular error:

$$\Delta\theta_k \cong \frac{\left\| \underline{\mathbf{a}}_h(\theta_k) \right\|^{-1} \Re e\left[\underline{\mathbf{b}}_h{}'^H(\theta_k) \mathbf{V}_n \mathbf{V}_n^H \Delta \underline{\mathbf{a}}_h(\theta_k) \right]}{\underline{\mathbf{b}}_h{}'^H(\theta_k) \mathbf{V}_n \mathbf{V}_n^H \underline{\mathbf{b}}_h{}'(\theta_k)} \quad (3.37)$$

Statistics of this error are calculated relatively to the characteristics of the perturbations affecting the array responses quantified by the matrices $\mathbf{C_{kkh}} = E[\Delta \underline{\mathbf{a}}_\mathbf{h}(\theta_k) \Delta \underline{\mathbf{a}}_\mathbf{h}(\theta_k)^H]$ and $\mathbf{D_{kkh}} = E[\Delta \underline{\mathbf{a}}_\mathbf{h}(\theta_k) \Delta \underline{\mathbf{a}}_\mathbf{h}(\theta_k)^T]$.

Denoting $\underline{\mathbf{g}}_\mathbf{k} = \mathbf{V}_n^H \underline{\mathbf{b}}'(\theta_k)$, we can finally express the mean square angular error for the heterogeneous array as:

$$E[\Delta\theta_k^2] = \frac{\Re e\left\{ \underline{\mathbf{g}}_\mathbf{k}^H \mathbf{V}_n^H \left(\mathbf{C_{kkh}} \mathbf{V}_n \underline{\mathbf{g}}_\mathbf{k} + \mathbf{D_{kkh}} \mathbf{V}_n^* \underline{\mathbf{g}}_\mathbf{k}^* \right) \right\}}{2 \left\| \underline{\mathbf{a}}_h(\theta_k) \right\|^2 \cdot \left(\underline{\mathbf{g}}_\mathbf{k}^H \underline{\mathbf{g}}_\mathbf{k} \right)^2} \quad (3.38)$$

3.4. *Numerical simulations*

3.4.1. Antenna arrays for HF direction finding

The active loop antenna is the standard sensor for HF direction finding system. Its size, small relatively to the wavelength guarantees an efficient spatial sampling of the incident waves and its load, being a low impedance, also reduces problems of dispersion which affect the high impedance preamplifiers of monopoles and dipoles.

Several loop antennas of the same type are classically associated in a circular uniform array for HF direction finding. The sensors are then equi-spaced along a circle and set up with the same orientation on an horizontal ground. This structure is considered in this section as the reference for an homogeneous array (fig. 6, left frame).

In the second array which is considered, the antennas are subject to a rotation of Nd degrees around a vertical axis every two positions within the array so that the structure becomes heterogeneous (fig. 6, right frame).

The spatial responses of the antennas ($F_n(\theta)$, n=1,…NC) are computed with an electromagnetic simulation software (NEC2D) coupled with a predictive model of the polarization emerging from the ionosphere (Erhel *et al.,* 2004).

The ground reflection is taken into account with an estimation of parameters conductivity and permittivity.

3.4.2. Perturbation model

In the expression of the perturbed steering-vector, errors in modulus and phase are separated. For a given angle of arrival (AOA) θ_k, the component of index n in this vector is expressed as:

$$\hat{\underline{\mathbf{a}}}(\theta_k)_n = (1 + \Delta m_{nk}) e^{j\Delta\phi_{nk}} \underline{\mathbf{a}}(\theta_k)_n \quad (3.39)$$

where Δm_{nk} and $\Delta\phi_{nk}$ are respectively the error son modulus and phase of component n.

The perturbation of the steering-vector can be written as:

$$\Delta \underline{\mathbf{a}}(\theta_k) = \hat{\underline{\mathbf{a}}}(\theta_k) - \underline{\mathbf{a}}(\theta_k) = \underline{\mathbf{dG_k}} \otimes \underline{\mathbf{a}}(\theta_k) \quad (3.40)$$

with

$$\underline{\mathbf{dG_k}} = \left[(1 + \Delta_{m1k}) e^{j\Delta\phi_{1k}} \ldots\ldots\ldots (1 + \Delta_{mNCk}) e^{j\Delta\phi_{NCk}} \right]^T$$

and $\otimes$ is the Schur-Hadamard product.
In the calculation of angular mean square errors for AOA θ_k, matrices C_{kk}, D_{kk}, C_{kkh} and D_{kkh} are then expressed as:

$$\begin{aligned} \mathbf{C_{kk}} &= \mathbf{P_1} \otimes \underline{\mathbf{a}}(\theta_k) \underline{\mathbf{a}}(\theta_k)^H \\ \mathbf{C_{kkh}} &= \mathbf{P_1} \otimes \underline{\mathbf{a}}_\mathbf{h}(\theta_k) \underline{\mathbf{a}}_\mathbf{h}(\theta_k)^H \\ \mathbf{D_{kk}} &= \mathbf{P_2} \otimes \underline{\mathbf{a}}(\theta_k) \underline{\mathbf{a}}(\theta_k)^T \\ \mathbf{D_{kkh}} &= \mathbf{P_2} \otimes \underline{\mathbf{a}}_\mathbf{h}(\theta_k) \underline{\mathbf{a}}_\mathbf{h}(\theta_k)^T \end{aligned} \quad 3.41$$

with

$$P_1(n,1) = E\left[\left((1 + \Delta m_{nk}) e^{j\Delta\phi_{nk}} - 1 \right) \left((1 + \Delta m_{lk}) e^{j\Delta\phi_{lk}} - 1 \right) * \right]$$

$$P_2(n,1) = E\left[\left((1 + \Delta m_{nk}) e^{j\Delta\phi_{nk}} - 1 \right) \left((1 + \Delta m_{lk}) e^{j\Delta\phi_{lk}} - 1 \right) \right].$$

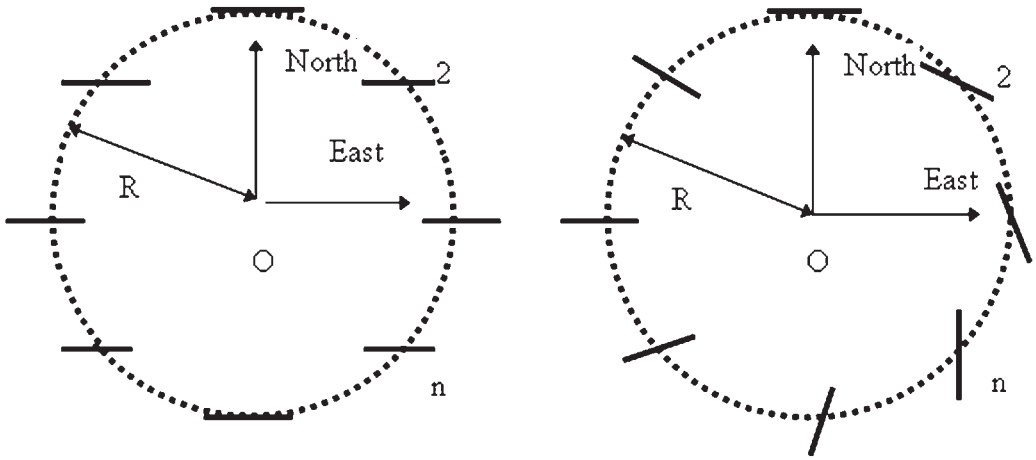

Fig. 6.a,b. Homogeneous circular array (left frame) and heterogeneous circular array (right frame).

For the numerical simulations presented in the next section, the assumptions concerning the perturbations are:

- independent perturbations of two different sensors
- Δm_n and Δg_n mutually independent for a given sensor
- Δm_n and Δg_n have zero mean values.

3.4.3. Comparison of robustness for two structures

The two circular arrays are characterized by geometrical parameters: number of sensors NC=10, diameter of each loop d=1.3m, array radius R=20m, inter-element rotation Nd=20° (heterogeneous case).

The scenario of the reception involves NS=2 signals with a carrier frequency fo=10 MHz, impinging on the arrays with azimuths of arrival Az_1=40° and Az_2=50°. The common elevation of arrival is assumed to be known. The signal to noise ratio (SNR) is equal to 12 dB and the B.T product (bandwidth by difference of group delays) is equal to 3.

Uncertainties with the same magnitude are assumed to affect the two array manifolds. For each sensor, the phase variation is uniformly distributed on the interval $[-\delta\phi_{max};+\delta\phi_{max}]$ with $\delta\phi_{max}$ = 15°. The modulus error is also uniformly distributed in an interval $[-\delta m_{max};+\delta m_{max}]$, δm_{max} being a variable parameter in the numerical simulation adjustable from 0 up to 40%.

The corresponding angular rms error affecting the azimuth estimation is computed for the two types of arrays according to the relations given in eq. 3.30 and eq. 3.38. The results are plotted in the left frame (homogeneous) and right frame (heterogeneous) of fig. 7.

For a given level of perturbation, the angular error is smaller when the direction finding is implemented on the heterogeneous array.

This observation remains systematically if the parameters of the scenario are modified in a large scale: number of incoming waves, directions of arrival, carrier frequency, signal to noise ratio.

Consequently, the heterogeneous array appears more robust than the equivalent homogeneous structure. This result however assumes the same magnitude of perturbation in the two array manifolds. This point needs further work as the model of steering-vector for the heterogeneous case requires the computation of the sensor spatial responses in addition to the classical geometrical phases: the level of uncertainty may increase with the number of parameters

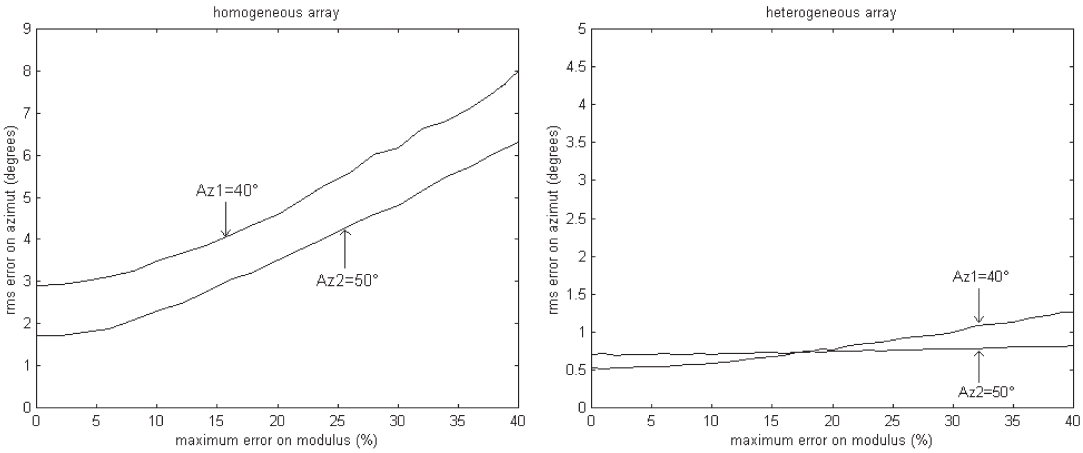

Fig. 7.a,b. RMS error, homogeneous array (left frame) and heterogeneous array (right frame).

present in the vector.

4. Concluding remarks

In order to realise increased channel capacity by means of a MIMO system, it is important that the signals received at each of the antenna elements of the receiver array from each of the elements of the transmitter array are adequately decorrelated. For the spaced heterogeneous antenna arrays described in this paper, this has been demonstrated experimentally to be the case. Furthermore, a preliminary assessment on the use of compact heterogeneous antenna arrays at the receiver has yielded encouraging results. Marked antenna orientation dependent and frequency dependent fading effects have been observed, and the prevailing modal structure of the ionosphere has been shown to have a key influence on the expected MIMO performance.

The correlation of multipath ionospherically reflected signals received at narrowly spaced antennas has been determined theoretically for different ionospheric conditions and paths using a wideband simulator based on a physical model including the effect of the frozen-in drift of ionospheric irregularities and both magneto-ionic modes. Conditions where the irregularities have a significant effect are likely to occur in the auroral, polar and equatorial regions. Each mode (*e.g.* 1Eo or 1Fx) can exhibit different "fading". Paths reflected from the *F* region generally show poorer correlation at spaced antennas than E region reflected paths. Calculations of estimated channel capacity show useful increased capacities even for quite high correlation levels of 0.8 or 0.9 for a 2x2 MIMO implementation.

In addition to the investigations on MIMO, the robustness of the MUSIC superresolution direction finding algorithm to modelling errors for both homogeneous and heterogeneous antenna arrays has been investigated through numerical simulations of trans-horizon scenarios in the HF band. The antenna array responses were calculated with the aid of electromagnetic simulation software with a deterministic model of the polarization of the radio waves emerging from the ionosphere and taking the effect of the ground into account. The results indicate higher robustness for the heterogeneous array for a given level of uncertainty than that for the homogeneous array. Modelling errors result classically from uncertainty in the position of the sensors, defaults in the electronic calibration or in the measurement of the electrical parameters of the antennas relative to the ground. For heterogeneous arrays, these uncertainties

are reinforced by the possibility of poor estimation of the polarization characteristics of the radiowave at the ionospheric exit point.

Acknowledgements

The authors are grateful to the EPSRC for their financial support of the experimental aspects of the HF-MIMO work. The collaboration between the UK and French groups in this investigation is facilitated through the EU COST 296 Action on the Mitigation of Ionospheric Effects on Radio Systems (MIERS).

REFERENCES

BRINE, N.L., C.C. LIM, A.D. MASSIE and W. MARWOOD (2006): Capacity Estimation for the HF-MIMO Channel, in *Proceedings of the Sixth Symposium on Radiolocation and Direction Finding*, (May 2006, Southwest Research Institute, San Antonio, Texas, USA).

ERHEL, Y., D. LEMUR, L. BERTEL and F. MARIE (2004): H.F. radio direction finding operating on a heterogeneous array: principles and experimental validation, *Radio-Science*, **39** (1), 1003-14.

GHERM, V.E., N.N. ZERNOV and H.J. STRANGEWAYS (2005): HF propagation in a wideband ionospheric fluctuating reflection channel: Physically based software simulator of the channel, *Radio Science*, **40** (1), doi:10.1029/2004RS003093.

GUNASHEKAR, S.D., E.M. WARRINGTON, S. SALOUS, S.M. FEENEY, H. ZHANG, N. ABBASI, L. BERTEL, D. LEMUR and M. OGER (2008): Early Results of Experiments to Investigate the Feasibility of Employing MIMO Techniques in the HF Band, in *Proceedings of the Loughborough Antennas and Propagation Conference 2008 (LAPC 2008)*, (March 2008, Loughborough, UK).

LOYKA, S.L. (2001): Channel capacity of MIMO architecture using the exponential correlation matrix, *IEEE Communications Letters*, **5** (9), 369-371.

MARCOS, S. (1998): *Les Méthodes à Haute Résolution: traitement d'antenne et analyse spectrale*, (Hermes, Paris).

PILLAI, S.U. (1989): *Array Signal Processing*, (Springer-Verlag, New York).

SCHMIDT, R.O. (1986): Multiple Emitter Location and Signal parameter Estimation, *IEEE Transactions on Antennas and Propagation*, AP-34 (33).

STRANGEWAYS, H.J. (2005): Determination of the correlation distance for spaced antennas on multipath HF links and implications for design of SIMO and MIMO systems, presented at the *2nd European Space Weather Week*, (Noordwijk, The Netherlands, 14-18 November, Published online).

STRANGEWAYS, H.J. (2006a): Estimation of signal correlation at spaced antennas for multi-moded ionospherically reflected signals and its effect on the capacity of SIMO and MIMO HF links, in *Proceedings of the 10th International Conference on Ionospheric Radio Systems, and Techniques*, (London, 18-21 July), 306-310.

STRANGEWAYS, H.J. (2006b): Determination of the capacity of ionospheric HF MIMO systems employing linear or planar arrays or co-located antennas, paper presented at *COST 296 workshop*, (Rennes, France 4-6 October 2006), published on the workshop CD-ROM.

STRANGEWAYS, H.J. (2006c): Determination of the correlation distance for spaced antennas on multipath HF links and implications for design of SIMO and MIMO systems, presented at the *1st European Conference on Antennas and Propagation (EuCAP)*, (Nice, France, 6-10 November 2006), published on Conference CD-ROM.